Botulinum toxin type B micromechanosensor

W. Liu*†‡, Vedrana Montana†‡§, Edwin R. Chapman¶, U. Mohideen*†‖, and Vladimir Parpura†§‖

Departments of *Physics and §Cell Biology and Neuroscience, and †Center for Nanoscale Science and Engineering, University of California, Riverside, CA 92521; and ¶Department of Physiology, University of Wisconsin, Madison, WI 53706

Edited by Ricardo Miledi, University of California, Irvine, CA, and approved September 9, 2003 (received for review June 20, 2003)

Botulinum neurotoxin (BoNT) types A, B, E, and F are toxic to humans; early and rapid detection is essential for adequate medical treatment. Presently available tests for detection of BoNTs, although sensitive, require hours to days. We report a BoNT-B sensor whose properties allow detection of BoNT-B within minutes. The technique relies on the detection of an agarose bead detachment from the tip of a micromachined cantilever resulting from BoNT-B action on its substratum, the synaptic protein synaptobrevin 2, attached to the beads. The mechanical resonance frequency of the cantilever is monitored for the detection. To suspend the bead off the cantilever we use synaptobrevin's molecular interaction with another synaptic protein, syntaxin 1A, that was deposited onto the cantilever tip. Additionally, this bead detachment technique is general and can be used in any displacement reaction, such as in receptor–ligand pairs, where the introduction of one chemical leads to the displacement of another. The technique is of broad interest and will find uses outside toxicology.

Botulinum neurototoxins (BoNTs) are the most potent of known toxins affecting humans (1). These toxins, which cause botulism, a dramatic and fatal form of intoxication in humans, are produced by the bacillus *Clostridium botulinum*. The three main forms of botulism are (*i*) food-borne botulism caused by ingestion of the BoNTs, (*ii*) wound botulism resulting from *Clostridium*-infected wounds, and (*iii*) infant botulism, caused by toxin production in infant intestines after consumption of the bacillus spores. Although cases of botulism are rare in the United States, they are all considered medical emergencies, resulting in death in ≈10% of cases (2). The recovery period can be many months and includes intensive care with extensive use of ventilators. BoNT types A, B, E, and F, which are toxic to humans (3), have distinctive geographic distributions (2). In the United States, type A is seen predominately west of the Mississippi River, type B in the Eastern states, whereas type E prevails in Alaska and the Great Lakes area. In Europe, meat products can be sources of type B, whereas vegetable produce in China can contain type A. Preserved fish in Japan, Russia, and Scandinavia can be a source of type E. Given the rapid increase in the international trade of food products, these geographical distributions of BoNT types will blur in the near future. Additionally, the potency and ease of distribution of BoNTs make them a threat as biological weapons. Thus, the Centers for Disease Control and Prevention (CDC) in Atlanta lists botulism as one of the six most dangerous bioterrorist threats (www.bt.cdc.gov/agent/agentlist-category.asp).

Vaccination against botulism is available for the three different serotypes of BoNTs affecting humans, but it requires multiple inoculations over an extended period to prevent intoxication (www.bt.cdc.gov/agent/agentlist-category.asp). Thus, it is not feasible to vaccinate entire populations, but rather the vaccine is used only for the protection of persons with a high risk of exposure. In addition to supportive therapy, if diagnosed early, botulism can also be treated immunologically by using an equine trivalent antitoxin (www.bt.cdc.gov/agent/agentlist-category.asp), or perhaps with recently developed oligoclonal antibodies (4). This treatment is effective if undertaken early in the course of intoxication, before the onset of symptoms. Thus, the early detection of the toxin is critical. The most direct way to detect BoNT is to inject human serum or stool into mice and look for signs of botulism (www.bt.cdc.gov/agent/agentlist-category.asp). This mouse bioassay can be performed at some state health department laboratories and the CDC. It is expensive, time-consuming, and subject to many legal and ethical constraints. There are attempts to replace the mouse bioassay by using the nematode *Caenorhabditis elegans* (www.griffin.peachnet.edu/cfs/research/ClostridiumResearch.html). In addition to the use of living animals in early detection, an enzyme-linked immunosorbent assay (ELISA) that taps into molecular actions of toxins was developed (5), speeding up the outcome of an assay from days needed in the case of bioassay to hours needed in ELISA. Here we report a BoNT-B sensor whose properties allow detection of BoNT-B within a few minutes.

Materials and Methods

Recombinant Proteins. Recombinant synaptobrevin 2 and syntaxin 1A were generated by using modified pET vectors as described elsewhere (6, 7), resulting in their cytoplasmic domains (amino acids 1–94 for synaptobrevin 2 and 1–265 for syntaxin 1A) tagged with six histidine residues (His_6) at their C termini. These proteins were purified by using nickel-Sepharose beads (Qiagen, Valencia, CA), and were quantified by SDS/PAGE and staining with Coomassie blue, with BSA as a standard. When subjected to SDS/PAGE followed by Western analysis, the proteins were loaded at 1 μg per lane. We probed membranes by using monoclonal antibodies against syntaxin 1 (clone HPC-1, Sigma), and against synaptobrevin 2 (clone 69.1, Synaptic Systems, Göttingen, Germany). Immunoreactive bands were detected by using enhanced chemiluminescence (ECL, Amersham Biosciences, Piscataway, NJ).

In experiments using the light chain of BoNT type B (BoNT-B; List Biological Laboratories, Campbell, CA) we incubated 200 ng of toxin with 1 μg of recombinant proteins in internal solution containing 250 μM zinc chloride at room temperature for 2 h, whereupon the reaction was stopped by adding 3× gel sample buffer. The internal solution contained (in mM) potassium gluconate, 140; NaCl, 10; and Hepes, 10 (pH 7.35; density = 1.02 g/ml).

Functionalization of Beads. We incubated 50 μl of nickel-agarose bead suspension (Qiagen, catalog no. 36111; 20–70 μm in diameter) with 18.75 μg of recombinant synaptobrevin 2-His_6 (0.17–0.33 mg/ml), for 1 h at room temperature. This bead/protein ratio ensured complete saturation of available nickel sites on beads. After three washes with internal solution, functionalized beads were kept at 4°C until used in experiments (up to 36 h). Before experiments the beads were applied to the glass coverslips that were mounted on metal disk atomic force mi-

This paper was submitted directly (Track II) to the PNAS office.

Abbreviations: BoNT, botulinum neurotoxin; BoNT-B, BoNT type B; AFM, atomic force microscope; Sb2-H6, synaptobrevin 2 with a C-terminal His_6 tag; Sx1A-H6, syntaxin 1A with a C-terminal His_6 tag.

‡W.L. and V.M. contributed equally to this work.

‖To whom correspondence may be addressed. E-mail: vlad@citrus.ucr.edu or umar.mohideen@ucr.edu.

croscope (AFM) sample holders or into glass-bottomed chambers for indirect immunochemistry.

Functionalization of Cantilevers. Triangular silicon nitride cantilevers (320 μm long; Digital Instruments, Santa Barbara, CA) with integral tips were coated with nickel by using a thermal evaporator. After nickel deposition, the tips were functionalized with syntaxin 1A-His_6 recombinant protein by incubating tips in solution containing proteins (0.16–0.24 mg/ml) for 3 h at room temperature. After this incubation the tips were rinsed three times with an internal solution. Functionalized tips were kept submersed in this internal solution in a humidified chamber at 4°C until used in experiments, up to 36 h.

Detection of Cantilever Resonance. We used Nanoscope E and associated equipment (Digital Instruments) for the attachment of the bead and optical detection of cantilever resonance. All experiments were carried out in a fluid cell that kept the hydration and osmotic properties of the sample. Positioning of the cantilever tip to attach the functionalized agarose bead and the raising of the cantilever with the attached bead were done with a micrometer *z*-positioner equipped with a stepper motor. The resonant frequency of the cantilever was excited by using a Wavetek frequency generator to drive a piezoelectric tube with ≈5-nm amplitude oscillations. A magnetic plate mounted on top of the piezo selectively excites the nickel-coated cantilever with the bead. This setup substantially reduces cantilever oscillations due to fluid cell resonances. Note that although the lowest free cantilever resonance in air is at 6.8 kHz, it is substantially modified to 1 kHz (≈70 Hz if bead attached) by immersion in internal solution. Hydrodynamic and viscous effects lead to an effective increase in the mass of the cantilever and corresponding lowering of the resonant frequency. Other peaks at 300 and 600 Hz, and the broad background at higher frequencies result from fluid and fluid cell dynamics. The maximal time resolution for individual amplitude spectra was 10 s. To reduce variability, 12 consecutive amplitude spectra were averaged for 2 min and used to present data.

In experiments using light chain of BoNT-B, internal solution was supplemented with BoNT-B (1–100 nM) and zinc chloride (250 μM). This solution was injected into the fluid cell by using microfluidic ports, resulting in 2.4- to 3-fold dilution of BoNT-B/Zn^{2+}. The final concentrations of BoNT-B/Zn^{2+} reported in this work were adjusted to accommodate dilution factors.

Indirect Immunochemistry. The presence of syntaxin 1A on functionalized tips and synaptobrevin 2 on functionalized beads was determined by indirect immunochemistry that was performed by using the same antibodies as in Western blot analysis. Cantilevers were incubated with the primary antibody for 1 h at room temperature, followed by triple washing with internal solution. The rhodamine-conjugated secondary antibody was applied and the preparation was incubated for 1 h at room temperature followed by a triple washout in internal solution. In experiments in which we increased the protonation of histidine residues, after functionalization of the cantilevers we incubated them for 30 min at room temperature with the modified internal solution containing (in mM) potassium gluconate, 140; NaCl, 10, and citric acid, 1 (pH 4.75).

For labeling of synaptobrevin 2 on beads, before the application of primary antibody, beads were incubated with 5% nonfat dry milk to prevent nonspecific binding. In experiments using the light chain of BoNT-B, we incubated functionalized beads before labeling procedure in an internal solution supplemented with 100 nM BoNT-B and 250 μM zinc chloride at room temperature for 2 h. Both tips and beads were kept hydrated until used in experiments.

Visualization for immunochemistry was done with an inverted

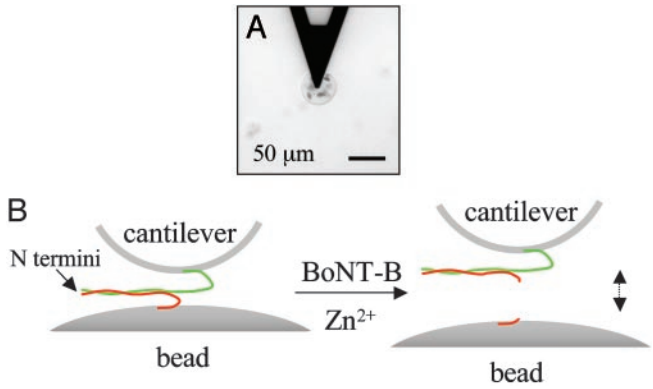

Fig. 1. (*A*) Top view of a cantilever with a syntaxin 1A-functionalized tip above a synaptobrevin 2-functionalized bead. (*B*) Recombinant synaptobrevin 2 (red) is attached to the nickel-coated bead surface through a histidine residue tag at its C terminus, leaving its N terminus free to interact with the N terminus of recombinant syntaxin 1A, which is similarly attached by means of a C-terminal histidine tag to the nickel-coated cantilever tip. The synaptobrevin 2–syntaxin intermolecular interaction leads to the bead's being tethered to the cantilever tip. BoNT-B in the presence of zinc ions (Zn^{2+}) cleaves synaptobrevin 2 in such manner that the short fragment of synaptobrevin 2 remaining on the bead has no ability to interact with syntaxin 1A on the cantilever tip, leading to the detachment of the bead from the tip (double-headed vertical arrow). The drawing in *B* is not to scale.

microscope (Nikon TE 300) equipped with wide-field epifluorescence (Opti-Quip, Highland Mills, NY; 100-W xenon arc lamp), and a standard rhodamine filter set (Chroma Technology, Brattleboro, VT). Images were captured through a ×20 air objective (Nikon) by using a CoolSNAP-HQ cooled charge-coupled device (CCD) camera (Roper Scientific, Tucson, AZ) driven by V++ imaging software (Digital Optics, Auckland, New Zealand). To reduce bleaching of the sample, an electronic shutter (Vincent Associates, Rochester, NY) was inserted in the excitation pathway and controlled by the software. Bright-field images were acquired with a green interference filter (GIF) inserted in the light path of a halogen lamp. All images presented in the figures represent raw data.

Results and Discussion

The sensor is based on the extraordinary force detection sensitivity available with microfabricated cantilevers (8–14). A schematic of the setup is shown in Fig. 1. The technique relies on the detection of agarose bead detachment from micromachined cantilever tips due to the enzymatic action of BoNT-B on its substratum, the synaptic protein synaptobrevin 2, also known as VAMP 2 (15, 16). Nickel-agarose beads were functionalized with recombinant synaptobrevin 2 conjugated to six consecutive His residues at its C terminus (Sb2-H6) (7). To suspend the bead off the cantilever tip we used synaptobrevin's molecular interaction with another synaptic protein, syntaxin 1A (17). We used commercially available AFM cantilevers that were nickel-coated and then functionalized them with a recombinant synaptic protein, syntaxin 1A conjugated to a His_6 tag at its C terminus (Sx1A-H6) (6). As both synaptic proteins were tagged at their C termini, their intermolecular N-terminal interactions are still allowed. The strength of this intermolecular interaction allowed us to keep the bead suspended off the cantilever tip until the delivery of BoNT-B. This toxin cleaves synaptobrevin 2 in such a manner that the bead containing a short fragment of synaptobrevin 2 detaches from the cantilever tip. Note that a single intermolecular syntaxin–synaptobrevin interaction is sufficient to hang a 41-μm-diameter bead off the cantilever tip, given the buoyancy of the bead in the fluid and the measured syntaxin–synaptobrevin interaction strength of 250 pN, when the AFM

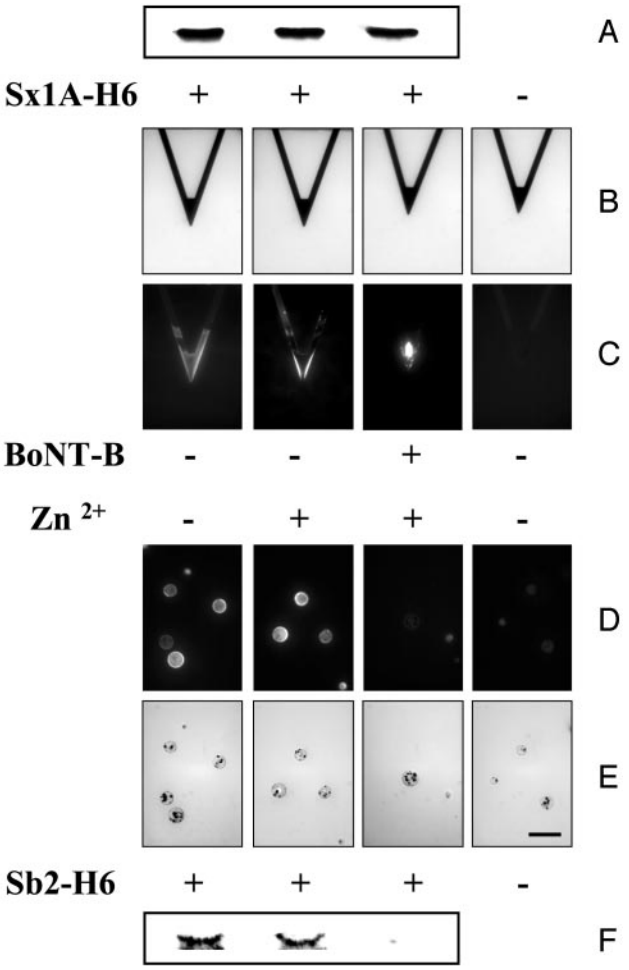

Fig. 2. BoNT-B in the presence of Zn^{2+} cleaves Sb2-H6, but not Sx1A-H6, as indicated by Western blot analysis (*A* and *F*). (*B*) Bright-field images of cantilevers that were subjected to indirect immunochemistry in *C*. Cantilevers incubated with Sx1A-H6 (+) were successfully functionalized as indicated by the positive immunoreactivity compared with the control cantilevers for which Sx1A-H6 was omitted from the incubation solution (−). Treatment of the functionalized cantilevers with Zn^{2+} alone or BoNT-B/Zn^{2+} did not reduce the syntaxin 1A immunoreactivity on cantilevers, consistent with the Western blot analysis in *A*. (*D*) Beads functionalized with Sb2-H6 (+) showed positive immunoreactivity compared with control beads for which Sb2-H6 was not attached to the bead (−). Treatment of the functionalized beads with Zn^{2+} alone or BoNT-B/Zn^{2+} indicated that BoNT-B/Zn^{2+} greatly reduced the synaptobrevin 2 reactivity on the bead (compare images in *D* and *E*), consistent with Western blot analysis in *F*. (*E*) Bright-field images of beads in *D*. (Scale bar in the right-most image in *E* indicates 100 μm for all images in *B–E*.)

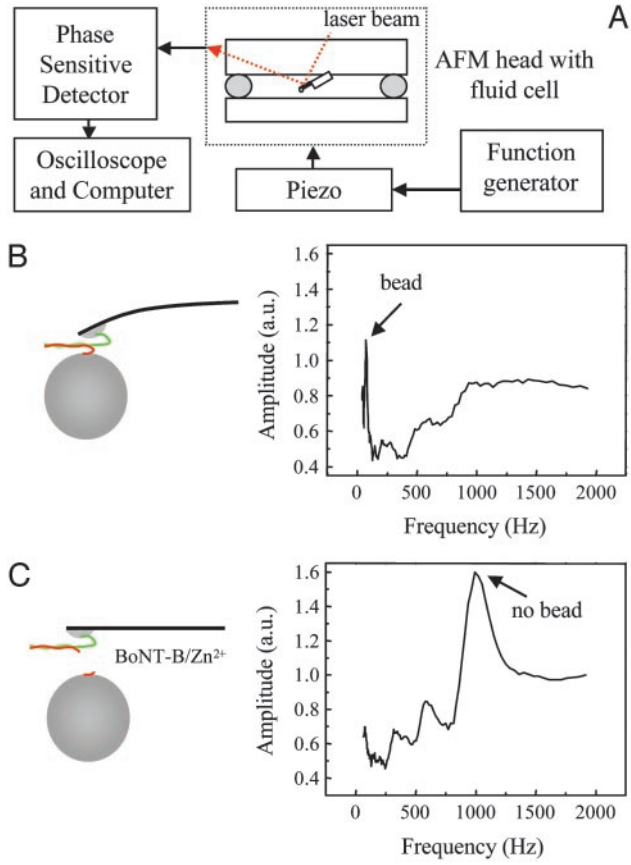

Fig. 3. (A) Schematic representation of the experimental setup used for the BoNT-B sensor. The syntaxin 1A-functionalized cantilevers with attached synaptobrevin 2-functionalized beads residing in the fluid cell of the AFM head were acoustically vibrated by means of a piezo driven by a function generator. The vibration amplitude of the cantilever was monitored by using the difference signal from a split photodiode system that collects the red laser beam reflected off the back of the cantilever. A phase-sensitive detector was used to measure the vibration amplitude as a function of the frequency, and the data were recorded in a digital oscilloscope and later exported to a computer. (*B*) A typical amplitude spectrum (*Right*) obtained for the cantilever with the bead attached (*Left*). The lowest-order resonance attributable to the combined cantilever–bead system is indicated by the arrow. (*C*) Three minutes after the injection of solution containing BoNT-B and zinc ions (BoNT-B/Zn^{2+}; 42 nM/104 μM) into the fluid cell, the sharp cantilever–bead resonance disappears, while the bare (no bead) cantilever resonance peak appears (*Right*, arrow), indicating the detachment of the bead from the cantilever. The vibration amplitude is expressed in arbitrary units (a.u.). Drawings are not to scale.

force spectroscopy technique (18) is used. Thus, this sensor methodology is highly sensitive, being based on the rupture of a single molecular bond (18–22). Chemically modified resonating cantilevers have been used as sensors primarily in gaseous and vacuum environments. They have relatively poor sensitivity in fluids because of hydrodynamic and viscous effects (23, 24). However, in the sensor technique reported here, even in fluids there is a large effective mass change of the cantilever due to the detachment of the bead, while it simultaneously retains high sensitivity.

Before attaching the recombinant syntaxin 1A and synaptobrevin 2 proteins to the cantilever tips and beads, respectively, we confirmed the specificity of BoNT-B to cleave Sb2-H6, but not Sx1A-H6, by incubating these proteins with BoNT-B and then subjecting them to SDS/PAGE (Fig. 2) (25). Subsequent Western blot analysis revealed that BoNT-B in the presence of zinc ions cleaved only Sb2-H6 (Fig. 2*F*), whereas Sx1A-H6 (Fig. 2A) was not affected by the action of this toxin. Additionally, BoNT-B alone, without externally added zinc ions, did not cleave Sb2-H6 (data not shown). These results are consistent with previous reports of toxin molecular actions (15, 16, 26). After this demonstration that our recombinant proteins show the same susceptibility to BoNT-B as the native proteins do, we proceeded to use these proteins in the functionalization of cantilever tips and beads.

Commercially available 320-μm-long triangular silicon nitride AFM cantilevers were coated with nickel by using a thermal evaporator, resulting in nickel films (thickness ≈150 nm) that are partially oxidized on exposure to air. After this nickel deposition, the tips were functionalized with Sx1A-H6 recombinant protein. Successful coupling was assessed by using indirect immunochem-

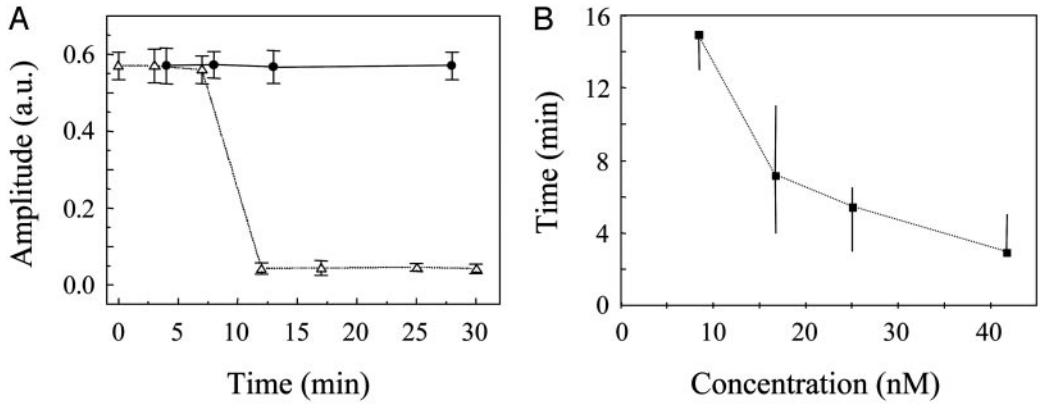

Fig. 4. Sensitivity of the BoNT-B micromechanosensor. (*A*) The change in the vibration amplitude of the cantilever loaded with the bead as a function of time. Time zero refers to the addition to the fluid cell of BoNT-B (17 nM; $n = 4$) in presence of Zn^{2+} (83 μM; △) or of Zn^{2+} alone (●; $n = 4$). A few minutes after the introduction of BoNT-B the cantilever–bead vibration amplitude drops to the background values, indicating the detachment of the bead. The vibration amplitude is expressed in arbitrary units (a.u.), and time is expressed in minutes. Points indicate mean values, and bars represent SEM. (*B*) The time in minutes taken for the detachment of the bead as a function of the BoNT-B concentration (8 nM, $n = 3$; 17 nM, $n = 4$; 25 nM, $n = 4$; and 42 nM, $n = 7$). Points indicate median values, and bars represent ranges. Medians are connected with a dotted line to indicate the trend.

istry. Monoclonal antibody against syntaxin 1A (27) revealed the presence of this recombinant protein only on functionalized cantilevers, but not on the control cantilevers from which recombinant proteins were omitted during the functionalization procedure (Fig. 2 *B* and *C*). Similarly, incubation of nickel-nitrilotriacetate (NTA) agarose beads with recombinant Sb2-H6 resulted in functionalization of beads (Fig. 2 *D* and *E*) as detected by the monoclonal antibody directed against the N terminus of synaptobrevin 2 (28). We incubated these functionalized cantilevers and beads with BoNT-B to check whether the toxin reacts with the immobilized recombinant proteins. Because BoNT-B is a zinc endopeptidase (26), and we showed the lack of its action on Sb2-H6 in the absence of externally added zinc, we added zinc ions to ensure BoNT-B reactions. We find that BoNT-B in the presence of zinc ions, but not zinc ions alone, causes the reduction in immunoreactivity of synaptobrevin 2-functionalized beads (Fig. 2 *D* and *E*), whereas we recorded no decrease in immunoreactivity of syntaxin 1A-functionalized tips (Fig. 2 *B* and *C*). However, when we decreased the pH from 7.35 to 4.75 to cause protonation of histidine residues, a treatment known to disturb the nickel–histidine coordination, we observed the reduction in immunoreactivity on AFM tips caused by detachment of previously immobilized recombinant proteins (data not shown). Taken together, the data indicate that BoNT-B specifically cleaves immobilized synaptobrevin 2, and that zinc ions do not significantly affect the nickel–histidine coordination.

After this initial confirmation of the protein deposition specificity and BoNT-B actions, we tested the feasibility of the proposed sensor. A schematic of the experimental setup is shown in Fig. 3*A*. The syntaxin 1A-functionalized cantilevers were loaded into an AFM head with the fluid cell containing internal saline. Next, synaptobrevin 2-functionalized nickel-agarose beads were introduced into the fluid cell. An optical microscope was used to locate the beads. The cantilever was lowered until its tip came into contact with a bead (Fig. 1*A*). This contact allowed the establishment of the syntaxin–synaptobrevin intermolecular interaction, leading to the attachment of the bead to the cantilever tip. The cantilever was then raised with the bead attached to the tip (Fig. 3 *A* and *B*). Next, the cantilever was vibrated by means of a piezo driven by a function generator. A magnetic plate mounted on top of the piezo was used to preferentially excite the nickel-coated cantilever/bead. This setup prevented the excitation of fluid cell resonances that normally arise from acoustic vibration (23, 24). The vibration amplitude of the piezo was around 5 nm. Frequencies from 10 Hz to 2 kHz were logarithmically scanned to locate the resonance frequency. The vibration of the cantilever was monitored by using the standard AFM optical lever technique. A phase-sensitive detector was used to measure the vibration amplitude of the cantilever as a function of the frequency. A typical amplitude spectrum obtained for the bead attached to the cantilever is shown in Fig. 3*B*. The lowest-order resonance attributable to the cantilever–bead system is shown with the arrow at 70 Hz. This cantilever–bead configuration resulting from the synaptobrevin–syntaxin intermolecular interactions was stable for several hours at room temperature (6 of 6 tested). Next we injected a solution containing BoNT-B (8–42 nM) and zinc ions (BoNT-B/Zn^{2+}) into the fluid cell. The bead detached (18 of 19 tested) from the cantilever after the introduction of the BoNT-B/Zn^{2+} (Figs. 3*C* and 4) but not after introduction of Zn^{2+} alone (0 of 6 tested) (Fig. 4*B*), resulting in the disappearance of the sharp cantilever–bead resonance peak at 70 Hz (Fig. 3*B*; arrow) and the appearance of the bare (no bead) cantilever resonance peak at 1.0 kHz (Fig. 3*C*; arrow). We optically confirmed the detachment of the bead. Note that the resonant frequencies of the cantilever were measured in a fluid environment and are thus modified by a factor of 6.8 from their vacuum values because of hydrodynamic and viscous effects (23, 24).

The sensitivity of the sensor to the BoNT-B concentration was next studied (Fig. 4). We applied various concentrations of BoNT-B, ranging from 0.3 to 42 nM, to our sensor. In Fig. 4*A* we show the change in the vibration amplitude of the cantilever loaded with the bead as a function of time. After delivery of Zn^{2+} (83–104 μM) alone the bead remained attached to the cantilever for times >30 min (Fig. 4*A*, ●). However, after introduction of BoNT-B/Zn^{2+} the amplitude reduced to the background value within minutes, indicating the detachment of the bead (Fig. 4*A*, △). The change in amplitude is abrupt and can be used as a digital trigger. The time taken for the detachment of the bead as a function of the BoNT-B concentration (Fig. 4*B*) indicates the reaction time of the system. The threshold of BoNT-B detection, defined as a bead detachment within 15 min after addition of BoNT-B, was 8 nM.

We have generated a sensor for the rapid and reliable detection of the neurotoxin BoNT-B. The sensor presently allows the detection of toxin at concentrations greater than 8 nM within minutes. Thus, while offering much better speeds of detection

compared with mouse assays and ELISAs, this sensor presently has lower sensitivity. The principle of the sensor is based on the change in the resonance frequency of a microfabricated cantilever resulting from the detachment of an attached bead as a consequence of the biochemical reactions carried out by a toxin. In the case of endopeptidase BoNT-B the reaction is related to the cleavage of the synaptic vesicle protein synaptobrevin 2. The cleavage of synaptobrevin 2 molecules leads to bead detachment and thus a large mass change to the cantilever–bead system. This change results in a clear and large resonant frequency shift even in a highly damped solution environment. This technique of frequency change from bead detachment is general and can also be implemented in displacement reactions, such as in receptor–ligand pairs, where the introduction of one molecule leads to the displacement of another. Thus, the sensor we have developed is of broad interest and will find use outside toxicology. It will also allow easy on-chip integration with electronics. Moreover, extensions using cantilever–bead arrays will substantially improve sensitivity, fidelity, and specificity, while also allowing parallel detection of multiple analytes.

This work was supported by National Institutes of Health Grants GM 56827 and MH 61876 (to E.R.C.), by a grant from the Milwaukee Foundation (to E.R.C.), by a National Science Foundation Nanoscale Exploratory Research Grant, by the National Institute of Standards and Technology through a Precision Measurement Grant (to U.M.), and by a grant from the Department of Defense/Defense Advanced Research Planning Agency/Defense Microelectronics Activity under Award No. DMEA90-02-2-0216 (to V.P. and U.M.). V.P. is supported by the Whitehall Foundation. E.R.C. is a Pew Scholar in the Biological Sciences.

1. Arnon, S. S., Schechter, R., Inglesby, T. V., Henderson, D. A., Bartlett, J. G., Ascher, M. S., Eitzen, E., Fine, A. D., Hauer, J., Layton, M., *et al*. (2001) *J. Am. Med. Assoc.* **285,** 1059–1070.
2. Berkow, R. & Fletcher, A. J., eds. (1992) *The Merck Manual of Diagnosis and Therapy* (Merck Research Labs., Rahway, NJ), 16th Ed.
3. Hatheway, C. L. (1990) *Clin. Microbiol. Rev.* **3,** 66–98.
4. Nowakowski, A., Wang, C., Powers, D. B., Amersdorfer, P., Smith, T. J., Montgomery, V. A., Sheridan, R., Blake, R., Smith, L. A. & Marks, J. D. (2002) *Proc. Natl. Acad. Sci. USA* **99,** 11346–11350.
5. Keller, J. E., Nowakowski, J. L., Filbert, M. G. & Adler, M. (1999) *J. Appl. Toxicol.* **19,** Suppl. 1, S13–S17.
6. Fasshauer, D., Antonin, W., Margittai, M., Pabst, S. & Jahn, R. (1999) *J. Biol. Chem.* **274,** 15440–15446.
7. Margittai, M., Otto, H. & Jahn, R. (1999) *FEBS Lett.* **446,** 40–44.
8. Hagleitner, C., Hierlemann, A., Lange, D., Kummer, A., Kerness, N., Brand, O. & Baltes, H. (2001) *Nature* **414,** 293–296.
9. Fritz, J., Baller, M. K., Lang, H. P., Rothuizen, H., Vettiger, P., Meyer, E., Guntherodt, H., Gerber, C. & Gimzewski, J. K. (2000) *Science* **288,** 316–318.
10. Jones, V. W., Kenseth, J. R., Porter, M. D., Mosher, C. L. & Henderson, E. (1998) *Anal. Chem.* **70,** 1233–1241.
11. Chen, F., Mohideen, U., Klimchitskaya, G. L. & Mostepanenko, V. M. (2002) *Phys. Rev. Lett.* **88,** 101801-1-4.
12. Drake, B., Prater, C. B., Weisenhorn, A. L., Gould, S. A., Albrecht, T. R., Quate, C. F., Cannell, D. S., Hansma, H. G. & Hansma, P. K. (1989) *Science* **243,** 1586–1589.
13. Mohideen, U. & Roy, A. (1998) *Phys. Rev. Lett.* **81,** 4549–4552.
14. Baselt, D. R., Lee, G. U., Hansen, K. M., Chrisey, L. A. & Colton, R. J. (1997) *Proc. IEEE* **85,** 672–680.
15. Jahn, R. & Niemann, H. (1994) *Ann. N.Y. Acad. Sci.* **733,** 245–255.
16. Schiavo, G., Benfenati, F., Poulain, B., Rossetto, O., Polverino de Laureto, P., DasGupta, B. R. & Montecucco, C. (1992) *Nature* **359,** 832–835.
17. Südhof, T. C., De Camilli, P., Niemann, H. & Jahn, R. (1993) *Cell* **75,** 1–4.
18. Florin, E. L., Moy, V. T. & Gaub, H. E. (1994) *Science* **264,** 415–417.
19. Merkel, R. (2001) *Phys. Rep.* **346,** 343–385.
20. Lee, G. U., Chrisey, L. A. & Colton, R. J. (1994) *Science* **266,** 771–773.
21. McKendry, R., Zhang, J., Arntz, Y., Strunz, T., Hegner, M., Lang, H. P., Baller, M. K., Certa, U., Meyer, E., Guntherodt, H. J. & Gerber, C. (2002) *Proc. Natl. Acad. Sci. USA* **99,** 9783–9788.
22. Oberhauser, A. F., Hansma, P. K., Carrion-Vazquez, M. & Fernandez, J. M. (2001) *Proc. Natl. Acad. Sci. USA* **98,** 468–472.
23. Schaffer, T. E., Cleveland, J. P., Ohnesorge, F., Walters, D. A. & Hansma, P. K. (1996) *J. Appl. Phys.* **80,** 3622–3627.
24. Walters, D. A., Cleveland, J. P., Thomson, N. H., Hansma, P. K., Wendman, M. A., Gurley, G. & Elings, V. (1996) *Rev. Sci. Instrum.* **67,** 3583–3589.
25. Parpura, V., Fang, Y., Basarsky, T., Jahn, R. & Haydon, P. G. (1995) *FEBS Lett.* **377,** 489–492.
26. Schiavo, G., Rossetto, O., Benfenati, F., Poulain, B. & Montecucco, C. (1994) *Ann. N.Y. Acad. Sci.* **710,** 65–75.
27. Barnstable, C. J., Hofstein, R. & Akagawa, K. (1985) *Brain Res.* **352,** 286–290.
28. Edelmann, L., Hanson, P. I., Chapman, E. R. & Jahn, R. (1995) *EMBO J.* **14,** 224–231.